



# Groove fibers based porous scaffold for cartilage tissue engineering application



Weiming Chen<sup>a</sup>, Binbin Sun<sup>a</sup>, Tonghe Zhu<sup>a</sup>, Qiang Gao<sup>a</sup>, Yosry Morsi<sup>b</sup>, Hany El-Hamshary<sup>c,d</sup>, Mohamed El-Newehy<sup>c,d</sup>, Xiumei Mo<sup>a,\*</sup>

<sup>a</sup> College of Chemistry, Chemical Engineering and Biotechnology, Donghua University, Shanghai 201620, China

<sup>b</sup> Faculty of Engineering and Industrial Sciences, Swinburne University of Technology, Hawthorn, Vic 3122, Australia

<sup>c</sup> Department of Chemistry, College of Science, King Saud University, Riyadh 11451, Saudi Arabia

<sup>d</sup> Department of Chemistry, Faculty of Science, Tanta University, Tanta 31527, Egypt

## ARTICLE INFO

### Article history:

Received 16 June 2016

Received in revised form 21 December 2016

Accepted 6 January 2017

Available online 7 January 2017

### Keywords:

Groove fiber

3D scaffold

Water absorption

Cartilage tissue engineering

Biomaterials

Elastic properties

## ABSTRACT

A porous scaffold was prepared by gelatin groove fibers for cartilage tissue engineering. The morphology of groove fibers and porous scaffolds were observed by scanning electron microscopy (SEM). The water absorption property of scaffolds was tested which demonstrated values as high as 1187%. The compressive mechanical property of scaffolds was also evaluated. In wet state, this scaffold exhibited elastic behaviour, and could bear 100 cycles compressive fatigue test. Moreover, this scaffold could promote rat chondrocyte and bone marrow mesenchymal stem cells (BMSC) proliferation. The findings indicate that such scaffold could be valuable candidates for cartilage tissue engineering.

© 2017 Elsevier B.V. All rights reserved.

## 1. Introduction

Articular cartilage has limited capacity for self-repair and regeneration after injury. Tissue engineering provides a promising strategy for cartilage regeneration [1]. Since tissue engineering was first developed in the early 1990s, a wide range of biomaterial scaffolds have been fabricated for tissue engineering application [2]. Ideal cartilage tissue engineering scaffold should have many characteristics, such as good water absorption, elasticity and biocompatibility. Water is important for maintaining the resiliency and lubrication of joint in cartilage [3], so scaffolds should have good water absorption property. Moreover, scaffolds should not only provide an environment for cells growth, but also be able to function for a certain period of time under load-bearing conditions [4]. Electrospinning is a convenient technology to prepare nanofibers for biomaterials [5–7] and as drug carriers [8], but most electrospun nanofibrous scaffolds are two-dimensional (2D) membranes. In this study, we present a novel 3D scaffold based on gelatin groove fiber and PLA fibers for cartilage tissue engineering application. To the best of our knowledge, short gelatin groove fibers were

firstly prepared by combining coaxial electrospinning and homogenization. In addition, by combining freeze-drying technique and crosslinking, the short gelatin groove fiber could form 3D scaffold with cellular structure. The obtained scaffold exhibited good water absorption and elastic property in wet state. In vitro study showed that this scaffold provided an environment for chondrocyte and BMSC to grow and proliferate. The groove fibers based porous scaffold are promising platforms for cartilage tissue engineering application.

## 2. Experimental section

### 2.1. Scaffold preparation

Fabrication of PLA/Gelatin nanofibers: Gelatin (Type A, MP Biomedicals, LLC) and PLA (Mw = 300 kDa, Medprin Regenerative Medical Technologies Co., Ltd) were separately dissolved in 1,1,1,3,3,3-Hexafluoro-2-propanol (>99%, darui finechemical Co., Ltd) with a gentle stirring for 12 h at room temperature. the concentration (w/v%) of gelatin and PLA were 12% and 8%, respectively. PLA solution was injected in core needle (inner diameter: 0.51 mm) and the flow rate of core solution was controlled at 1 ml/h, gelatin solution was injected in shell needle (inner diameter: 1.69 mm)

\* Corresponding author.

E-mail address: [xmm@dhu.edu.cn](mailto:xmm@dhu.edu.cn) (X. Mo).

and the flow rate of shell solution was controlled at 5 ml/h. A high voltage of 13 kV and collecting distance at 15 cm were applied for the electrospinning process. The nanofibers were prepared at room temperature with a relative humidity of 45–65%.

**Fabrication of 3D scaffold:** 5 g PLA/Gelatin nanofibers mats were cut into fragments and put in 100 ml tert-butanol, which were then homogenized for 10 min at 9,000 rpm by an IKA T18 homogenizer. The obtained dispersions were poured into cylindrical mould, frozen in  $-20\text{ }^{\circ}\text{C}$  for 0.5 h, and then freeze dried for 24 h to obtain the uncrosslinked 3D scaffold. The uncrosslinked sample was heated at  $180\text{ }^{\circ}\text{C}$  in air for 2 h to obtain heat treated scaffold (HS). HS were immersed in water for 2 h, frozen in  $-20\text{ }^{\circ}\text{C}$  for 0.5 h, and then freeze dried for 24 h to obtain the heat and water treated scaffold (HWS).

## 2.2. Characterization

The surface morphology of PLA/Gelatin nanofibers membrane, gelatin groove fiber, uncrosslinked scaffold, HS, and HWS were sputter coated with gold and observed by SEM (TM-1000, Hitachi) at an accelerating voltage of 5 kV. The core-shell structure of PLA/Gelatin nanofiber was observed using a Transmission Electron Microscopy (TEM, H-800, Hitachi), the nanofibers were collected on carbon-coated Cu grids for analysis. Water absorption capacity of HWS was studied according to the reported method [9]. The compressive mechanical property of uncrosslinked sample, HS, and HWS ( $n = 3$ , diameters of 10 mm and height of 13 mm) in dry state were tested by Instron 5969 testing system. The compression strain-stress curves of HWS in wet state with compression strain ( $\varepsilon = 60\%$  and  $80\%$ ) were measured. In addition, a 100 cycle loading-unloading fatigue test (wet HWS) with compression strain ( $\varepsilon = 60\%$ ) was also obtained.

Chondrocyte and BMSC were separately cultured in DMEM/F12 complete medium. A cell number of  $2 \times 10^4$  viable Chondrocyte and BMSC were separately seeded into HWS, and then incubated at  $37\text{ }^{\circ}\text{C}$  in a humidified atmosphere containing  $5\%$   $\text{CO}_2$ . The proliferation of BMSC on the scaffold was evaluated with MTT assay after 1, 3, 5, and 7 days of culture. The morphologies of chondro-

cyte and BMSC on the scaffold were studied by SEM after 5 days culture. The viabilities of chondrocyte and BMSC on the scaffold were detected using Live & Dead cell viability assays after 5 days of culture, and observed by optical microscope (TS100, Nikon). For biodegradability study, uncrosslinked sample and HWS were placed in phosphate buffered solution at  $37\text{ }^{\circ}\text{C}$ . The percentage of mass remaining after degradation was tested within the scheduled time (2 months).

## 3. Results and discussion

The synthetic steps of 3D scaffold was showed in Fig. 1a. PLA/Gelatin nanofibers with core-shell structure could be prepared by coaxial electrospinning (Fig. 1b). The diameter of nanofibers ranged from  $0.5\text{ }\mu\text{m}$  to  $3.6\text{ }\mu\text{m}$ , and the average diameter was about  $1.71 \pm 0.526\text{ }\mu\text{m}$ , which could be observed in Supporting information (Fig. S1b). By using high-speed homogenizer, the nanofibers membrane (Fig. 1c) pieces were dispersed into short gelatin groove fibers and PLA fibers (Fig. 1d). Gelatin fibers were more brittle than PLA, under the action of mechanical agitation, gelatin fibers fractured into groove fibers, and inner PLA fiber was displaced from the PLA/Gelatin fiber. The mixture of gelatin groove fibers and PLA fibers could be observed in Supporting information (Fig. S1a). The average length of gelatin groove fibers was  $14.6\text{ }\mu\text{m}$  (Supporting information, Fig. S1c). The obtained dispersions were poured into cylindrical mould, frozen and freeze-dried to obtain uncrosslinked sample. In this study, the scaffold was crosslinked by heat treatment. After heat treatment, interchain crosslink and amide formation could be formed on gelatin by dehydration, which made gelatin be insoluble. It should be noted that no toxic agent was used for crosslinking the scaffold. Moreover, Pores could be observed and were randomly distributed in the uncrosslinked sample (Fig. 1f), HS (Fig. 1g), and HWS (Fig. 1h). Fig. 1e shows a digital photo of resulting HWS.

As shown in Fig. 2a, the HWS showed excellent water absorption performance, and could achieve the maximum water absorption (1187%) less than 10 minutes after it came in contact with the water. The scaffold also exhibited reversible water absorbency

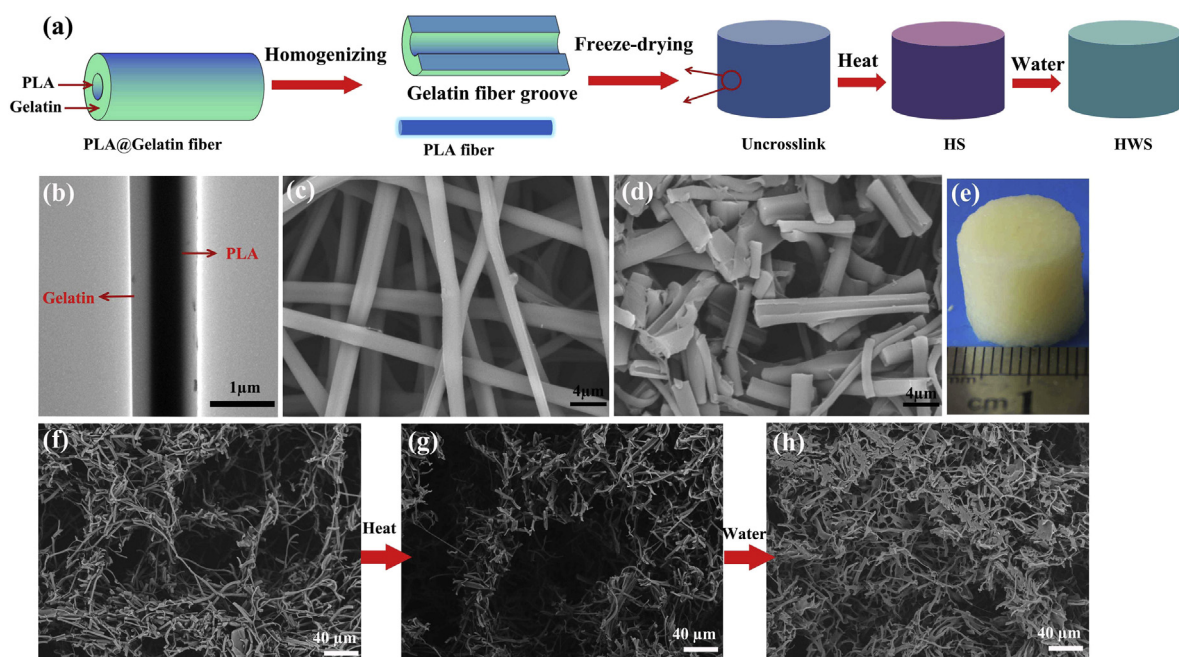


**Fig. 1.** (a) Schematic illustration showing the preparation of gelatin groove fiber and 3D scaffold, (b) TEM image of PLA/Gelatin nanofiber, (c) SEM image of PLA/Gelatin nanofibers membrane, (d) SEM image of gelatin groove fibers, (e) digital photo of HWS, (f), (g), and (h) were SEM images of uncrosslinked sample, HS, and HWS, respectively.

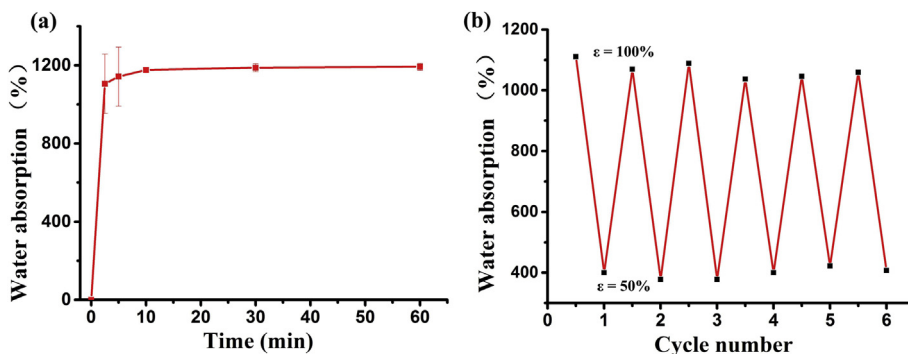


Fig. 2. (a) The water absorption behavior of HWS, (b) water absorption ratio of scaffolds at different compressive strain ( $\epsilon = 100\%$  and  $50\%$ ).

(Fig. 2b). Most of absorbed water would be squeezed out from the scaffold due to a compressive strain of 50%. After the scaffold was immersed in water, it would absorb water again.

The compressive strength of uncrosslinked scaffold would increase by heat treatment or heat & water treatment (Fig. 3a). The Young's modulus of uncrosslinked sample, HS, and HWS were  $30.11 \pm 2.33$ ,  $217.43 \pm 38.69$ , and  $1369 \pm 66.91$ , respectively (Fig. 3b). The results indicated that high temperature could crosslink gelatin by dehydration, which increased the compressive strength of scaffold. In addition, after the HS was treated with water, the nanofibers would stick together (Fig. 1h), that might be the reason why HWS possessed greater strength than HS. HWS also

exhibited elastic property in wet state. Fig. 3c showed that the scaffold could support 60% or 80% compressive strain and recover its original shape after the compressing force was released. A cyclic compression test with 100 loading-unloading fatigue cycles with 60% strain was also performed in this study (Fig. 3d). After 100 cycles compressive fatigue test, no significant strength decrease was observed, which indicated the outstanding cycling performance of the scaffold.

Both chondrocyte (Fig. 4a) and BMSC (Fig. 4c) were able to adhere on the scaffolds, which were evaluated by SEM. Live & dead assays (Fig. 4b and d) showed that live cells (green) grew much more than dead cells (red), indicating the excellent cell viability.

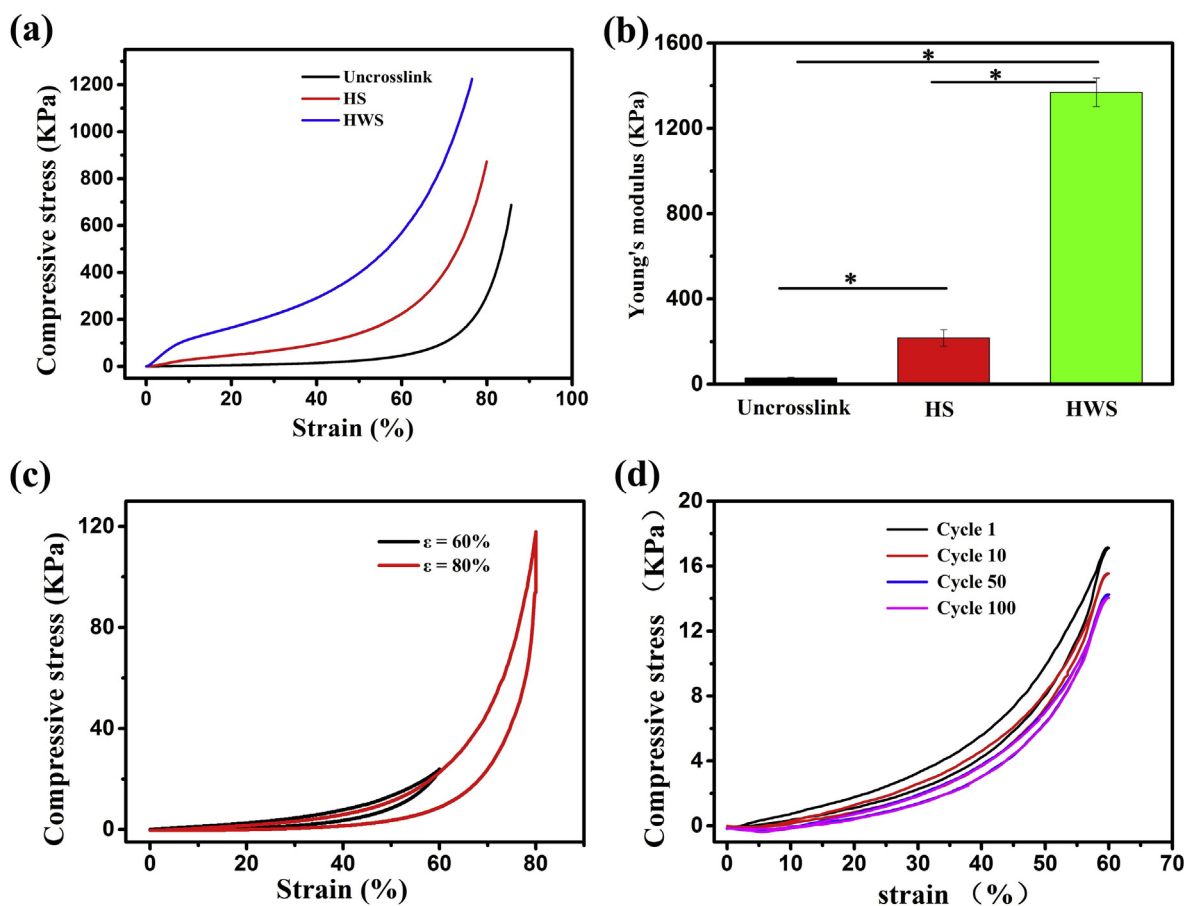
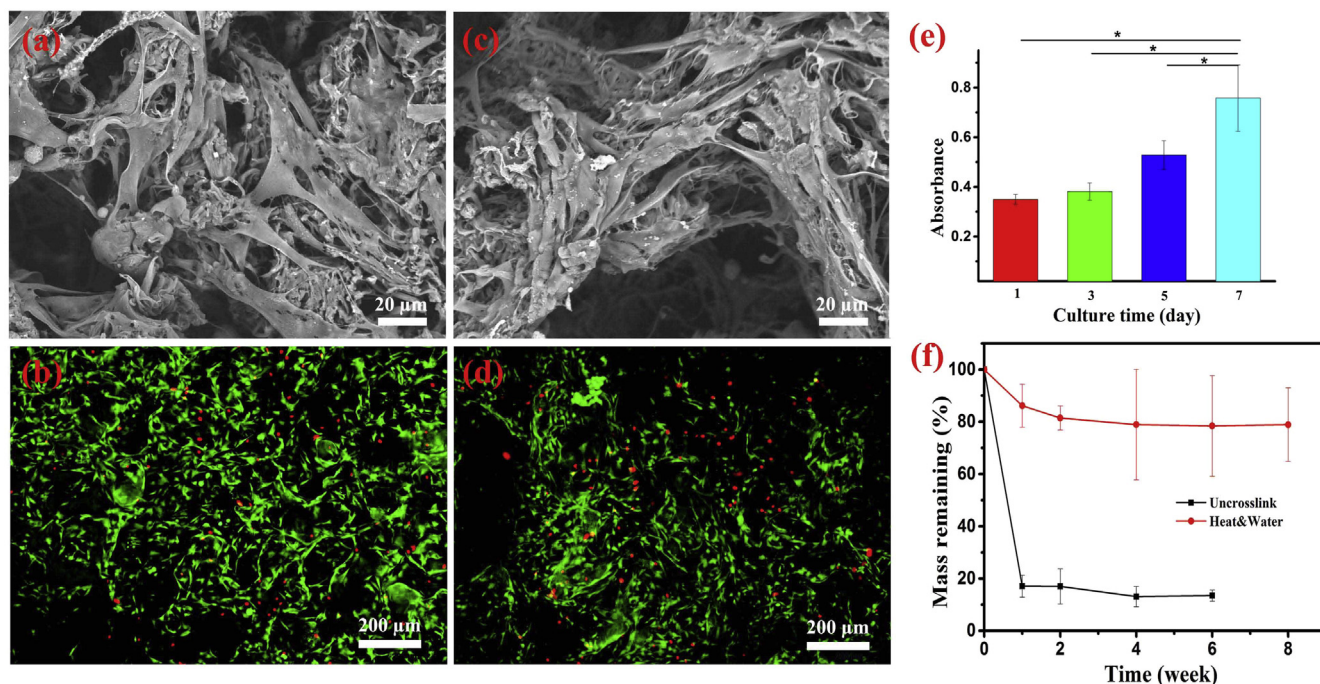


Fig. 3. Compressive stress-strain curves (a) and Young's modulus (b) of the uncrosslinked sample, HS, and HWS. (c) Compressive stress-strain curves of the HWS under two compressing and releasing cycles ( $\epsilon = 60\%$  and  $80\%$ ). (d) 100 cycles compressive fatigue test of HWS ( $\epsilon = 60\%$ ). The samples in (a) and (b) were tested in dry state, samples in (c) and (d) were tested in wet state.



**Fig. 4.** SEM image (a) and fluorescence micrograph (b) of chondrocyte seeded on HWS after 7 days of culture. SEM image (c) and fluorescence micrograph (d) of BMSC seeded on HWS after 7 days of culture. (e) BMSC proliferation test on HWS ( $n = 3$ , \* indicates statistically significant difference,  $p < 0.05$ ). (f) In vitro degradation of uncrosslinked sample and HWS. (Live and dead cells dyed green and red, respectively).

MTT assay (Fig. 4e) revealed that BMSC proliferation was significant after 7 days of culture. Briefly, the 3D scaffolds provided an environment for cells to proliferate. Uncrosslinked scaffolds exhibited a high rate of biodegradation (Fig. 4f). However, HWS could retain about 78% mass after two months of degradation in vitro. Biodegradation test indicated that heat & water treatment was an effective procedure for crosslinking the scaffolds.

#### 4. Conclusions

A novel gelatin groove fiber was introduced, and gelatin groove fibers and PLA fibers were used to fabricate 3D scaffolds. Heat and water treatment were used as crosslinking process to obtain stable scaffolds with enhanced compressive strength and long degradation time. The 3D scaffolds exhibited excellent water absorption performance, and elastic property in wet state. Moreover, it was also found that the scaffolds were able to well support the growth and proliferation of chondrocyte and BMSC, suggesting that the 3D scaffolds would have potential for cartilage tissue engineering.

#### Acknowledgements

This study was supported by National Nature Science Foundation of China (31470941, 31271035), Science and Technology Commission of Shanghai Municipality (15JC1490100, 15441905100), the Fundamental Research Funds for the Central Universities

(CUSF-DH-D-2016021). The authors extend their appreciation to the International Scientific Partnership Program ISPP at King Saud University for its funding research through (ISPP-0049).

#### Appendix A. Supplementary data

Supplementary data associated with this article can be found, in the online version, at <http://dx.doi.org/10.1016/j.matlet.2017.01.027>.

#### References

- [1] J. Wang, Q. Yang, N. Cheng, X. Tao, Z. Zhang, X. Sun, Q. Zhang, *Mater. Sci. Eng. C* 61 (2016) 705–711.
- [2] T.G. Kim, H. Shin, D.W. Lim, *Adv. Funct. Mater.* 22 (12) (2012) 2446–2468.
- [3] H.J. Mankin, A. Thrasher, *J. Bone Joint Surg. Am.* 57 (1) (1975) 76–80.
- [4] D.W. Huttmacher, *Biomaterials* 21 (24) (2000) 2529–2543.
- [5] P. Mehta, R. Haj-Ahmad, M. Rasekh, M.S. Arshad, A. Smith, S.M.V.D. Merwe, L. Xiang, M.W. Chang, Z. Ahmad, *Drug Discovery Today* (2016), <http://dx.doi.org/10.1016/j.drudis.2016.09.021>.
- [6] Z. Ekemen, H. Chang, Z. Ahmad, C. Bayram, Z. Rong, E.B. Denkbass, E. Stride, P. Vadgama, M. Edirisinghe, *Biomacromolecules* 12 (12) (2011) 4291–4300.
- [7] D.M. Yunus, Z. Ahmad, A.R. Boccaccini, *J. Chem. Technol. Biotechnol.* 85 (6) (2010) 768–774.
- [8] M. Rasekh, C. Karavasili, Y.L. Soong, N. Bouropoulos, M. Morris, D. Armitage, X. Li, D.G. Fatouros, Z. Ahmad, *Int. J. Pharm.* 473 (1–2) (2014) 95–104.
- [9] S.K. Ramadass, S. Perumal, A. Gopinath, A. Nisal, S. Subramanian, B. Madhan, *ACS Appl. Mater. Interfaces* 6 (17) (2014) 15015–15025.